Journal of Engineering and Applied Sciences 13 (24): 10436-10441, 2018
ISSN: 1816-949X

A Low Profile Solar Reflectarray Antenna Element with Enhanced Bandwidth

A. Selamat, M. Ramli, N. Misran, M.F. Mansor and S.H. Zaidi
Centre of Advanced Electronic and Communication Engineering,
Faculty of Engineering and Built Environment, Universiti Kebangsaan Malaysia,
43600 Bangi, Selangor, Malaysia

Abstract: A low profile solar cell integrated with reflectarray element composed of multilayer materials is presented in this study. A unit cell consist of triangular loop shape element is varied in size to get the required phase range. Some modification is then introduced to the triangular loop element aimed to optimize the bandwidth. A wide bandwidth range over 15% has been achieved. A prototype of the solar reflectarray cell was fabricated and measured. The measured results show good agreement with simulation. The element is designed to be operated at K_u-band frequency and formed a solar reflectarray antenna used for terrestrial applications.

Key words: Bandwidth, reflectarray, triangular loop, solar cell, measured results, terrestrial applications

INTRODUCTION

Passive or Reconfigurable reflectarray (RA) antenna has the potential to replace bulky conventional parabolic antenna (Ramli *et al*., 2014). Possessing a flat surface has facilitated the antenna to be installed either on the wall, on the roof of a house or business premises. The flat surface also provides many benefits including the ability to be integrated with solar panel (Zawadzki and Huang, 2000). Light weight and inexpensive to be manufactured are also the advantages of the RA. Although, many researchers have done RA and Solar Cell (SC) integration but bandwidth limitation of the RA antenna still occur and need to be addressed. A study on the integration of both RA and SC has been discussed in Dreyer *et al*. (2014) where the phase range results obtained did not reach 300° to cover the phase shift. It also has been demonstrated that a larger phase range allow to improve antenna bandwidth (Encinar and Zornoza, 2003). Therefore, broader phase range has to be achieved in order to enhance bandwidth.

Several phasing techniques on regular RA are available (Encinar and Zornoza, 2003; Misran *et al*., 2003; Carrasco *et al*., 2006; Oh *et al*., 2009) and can be applied to improve the bandwidth and phase range performance of this RA and SC integration. The techniques included the use of a multi-layered substrate (Encinar *et al*., 2003; Misran *et al*., 2003) the use of delay lines (Carrasco *et al*., 2006), slotted ground plane (Oh *et al*., 2009). Recently, an optimization process has been employed in some studies and phase ranges exceeding 300° have been reported (Chen *et al*., 2013; Li *et al*., 2009, 2011). The optimization process involves direct modification to the elements of the regular RA. A study involving elements with the I-shaped and encompassed with ring loop has been reported to produce phase range exceeding 360° with bandwidth of 15.2% (Chen *et al*., 2013). In the study, each element was tuned to match the required phase delay on two edge frequencies to obtain a fixed phase difference between two adjacent elements in the optimized band. In addition, phase range exceeding 360° has also been successfully produced using parasitic bipolar (Li *et al*., 2009). A unit-cell consisting of one main dipole element was flanked by parasitic bipolar and resized to produce broadband RA antenna. Bandwidth of 14.1% has been achieved in the study. Furthermore, study involves the use of a gap as an optimization methods have also been reported to generate phase range exceeding 360° (Li *et al*., 2011). The introduction of gap to the regular RA element caused the element's properties to resemble a capacitor and was capable of producing varies reflection phase to generate broadband antenna.

In this study, a novel triangular loop shape element is presented for solar RA antenna. On the first study, the triangular loop element has been resized but still retaining the triangular loop shape. Phase range exceeding 300° has been successfully produced. Subsequently, an optimization process has been employed in second study by applying some modification to the triangular loop shape element. As a result, the output bandwidth exhibited >15% with consistent phase range performance (>300°). A prototype of the solar RA element has been fabricated and measured and the results obtained are in line with the simulated results.

Corresponding Author: A. Selamat, Centre of Advanced Electronic and Communication Engineering,
Faculty of Engineering and Built Environment, Universiti Kebangsaan Malaysia, 43600 Selangor, Malaysia

MATERIALS AND METHODS

Triangular loop element with integrated solar panel: The single element structure as shown in Fig. 1 is composed of several layers of material which combined together to form a solar antenna. The layers comprise of a Kapton film, a glass layer, a silicon layer and copper layer. The Kapton film which is stacked on a glass layer plays the main role on the antenna part. It comprises of copper and polyimide material. The film exhibited conductivity value, σ of 5.8×10^7 sec/m. The copper on top of the polyimide material was shaped into triangular loop shape, thus, it operates at dual frequencies. The triangular loop element which was originally shaped with triangular patch has been selected as the radiating elements to facilitate more sunlight penetration on the first layer and irradiation to the silicon layer. This is consistent with the objective of the designed antenna to work as a solar RA antenna. The glass layer with conductivity value, σ 1×10-12 sec/m was then supported by a silicon layer and ended with a copper layer which acts as a ground plane. Monocrystalline has been selected as the type of Silicon layer which plays the major role on the solar part. The semiconductor material formed of p-layer and n-layer will generate potential different when exposed directly to the sunlight.

Triangular loop element with varied sizes: In the early design stage, phasing scheme of the triangular loop shape element has been set using element of varied sizes. The size of triangular loop element is altered by the ratio of 1:1 for each side. The side length "o" has been selected to be the tuned parameter in this experiment. The length is altered from 4.8-9.6 mm. The changes apply to the size of the triangular loop element only and keep everything else constant as in Table 1.

The element has been simulated using CST Microwave Studio Software with normal incidence plane wave. Figure 2 shows the phase response due to changes in the size of element. It is observed that the change in resonant frequency is noticeable starting from 13.2-18 GHz in line with changes in length of "o" ranging from 4.8-9.6 mm. The situation occurs due to the modification made in the dimensions of element which in turn changes the surface current flow on the element.

Figure 3 shows current distribution on the surface of triangular loop element. When the length "o" was set to 8 mm, the surface current is reaching the peak level and marked 209 A/m which worked at both 13.7 and 15.5 GHz frequencies. But when the length was changed to 6.4 mm, the surface current becomes low and drop to 60.9 A/m and has been operated at 14.3 and 16.9 GHz. It is observed that when the triangular loop element is changing in term of

Table 1: Dimension of each layer

Layer dimension	X (mm)	Y (mm)	Thickness (mm)
Periodicity	10	10	t = 4.351
Kapton film	-	-	t_1 = 0.151
Silica glass	10	10	t_2 = 3.900
Silicon solar cell	10	10	t_3 = 0.200
Copper (ground)	10	10	t_4 = 0.100

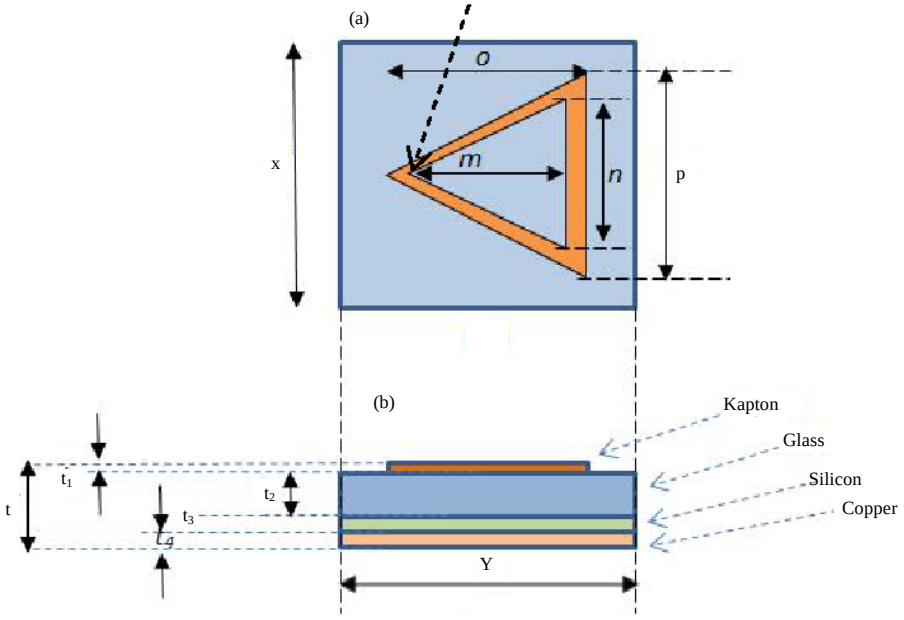

Fig. 1: Element structure: a) Top view and b) side view (length X = length Y)

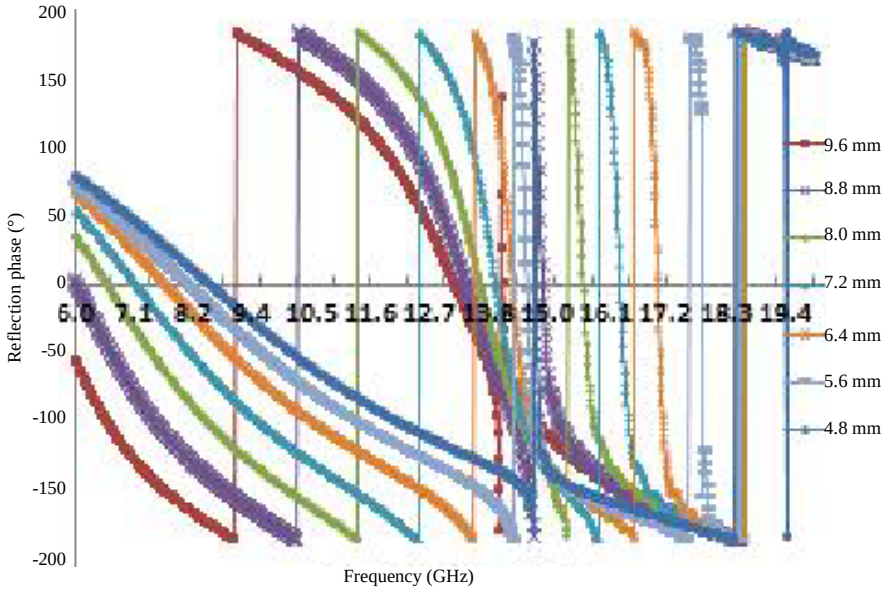

Fig. 2: Reflection phase response at different length of 'o'

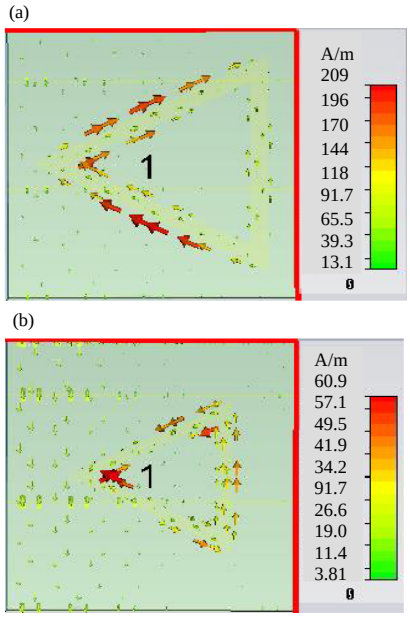

Fig. 3: Surface current distribution: a) o = 8 mm and b) o = 6.4 mm

surface size, the resonant frequency is also changing. This feature causes a phase change to the element and further impact the RA antenna phase range.

A linear phase range graph obtained from the designed element which operates at 13.7 GHz frequency is shown in Fig. 4. The graph is formed by the data obtained from different phases occurred due to the changes in the triangular loop element's surface as

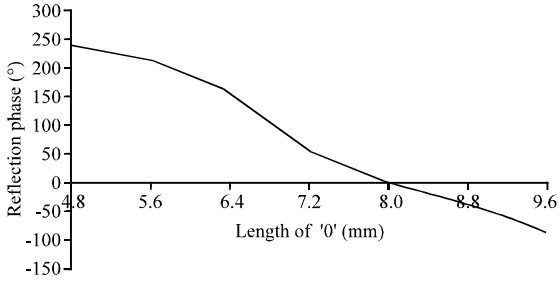

Fig. 4: Simulated reflection phase with respect to different length of 'o' at 13.7 GHz

discussed earlier. The linear phase range is observed to achieve 326°. Although, the result has not fulfilled the main RA requirement phase range which atleast reaches 360° but the achieved phase range is sufficient to reflect the incoming signals from front and has made the antenna works as a RA antenna. Meanwhile, the obtained bandwidth is observed to be <15% around 14.5%.

Triangular loop element with length 'm' and 'n' modification: An optimization of the triangular loop element has been conducted to produce wider bandwidth result. The optimization involves altering the length of 'm' and 'n'. Outer lengths of the triangular loop element are maintained where the length of "o" remains at 8 mm thus, it operates at both 13.7 and 16 GHz frequencies. The length 'm' is perpendicular to the base of the inner triangular loop element as shown in Fig. 1. The length is varied by changing one of its ends (peak of inner

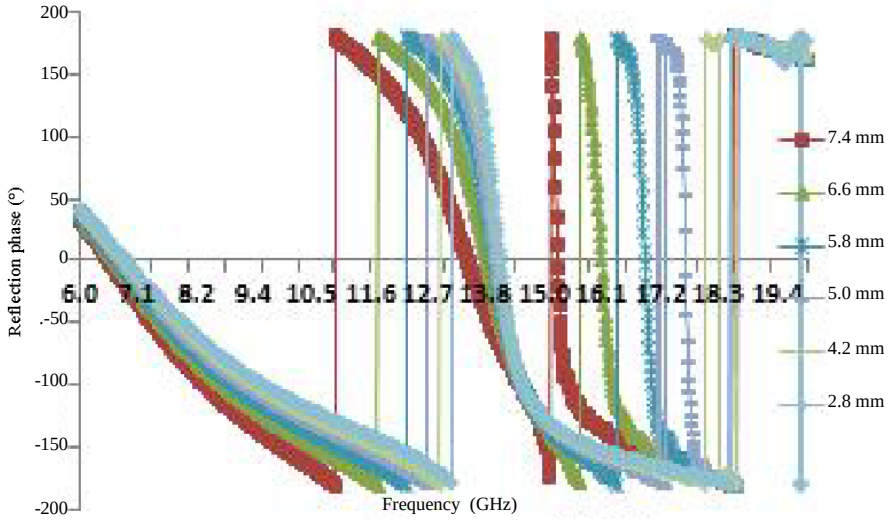

Fig. 5: Simulated reflection phase with respect to different length of 'o' at 13.7 GHz

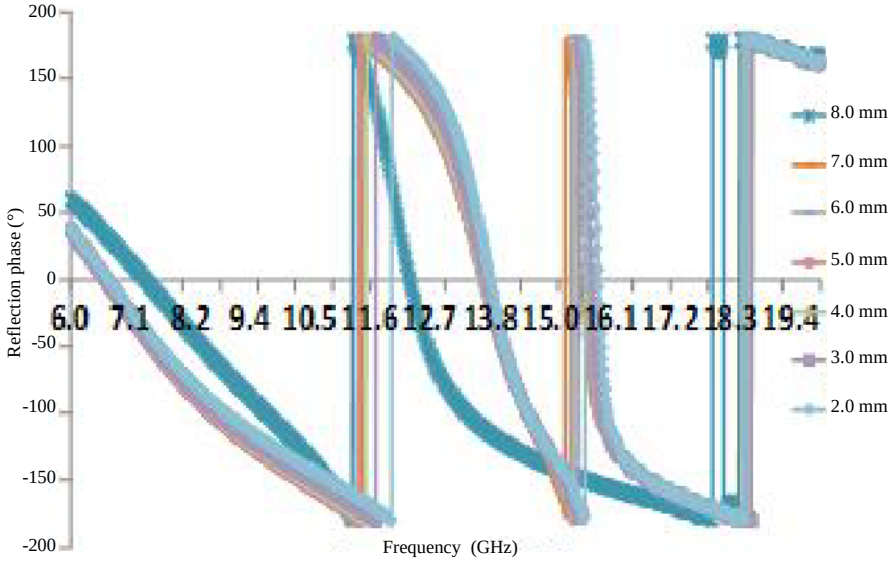

Fig. 6: Reflection phase response at different length of 'n

triangular shape, marked with 'r') while the other end remains fixed (base of inner triangular shape). Position of point 'r' is varied, so that, the length 'm' will vary from 2.8-7.4 mm. Changes in resonant frequency for each variation of position 'r' can be seen from the graph as shown in Fig. 5. It is observed that a longer length corresponds to a smoother resonance while a shorter length contributes to a higher slope. It is also, seen that the reflection phase is better when the length was set at 6.6 mm which works at dual frequencies within K_u-band.

Observation is also done by altering the length of 'n' ranging from 2-8 mm. This variation process of increasing or decreasing the length of 'n' is actually to describe about pillars of triangular loop element to be thinner or thicker. The effects are shown in Fig. 6. It is found that not much change occur to the reflection phase when length 'n' was varied from 2-7 mm. Most resonance occurs at 13.6-13.8 GHz. But once the length 'n' was set at 8 mm, the resonance frequency occurred at 12.3 GHz. This is due to copper lost on some area of the triangular loop element, hence, dropping the surface current of the triangular element and at the same time changing its resonance frequency. It is also, demonstrated that the reflection phase performance is smoother with wider bandwidth (17.5%) when the length 'n' was set at 6 mm.

Table 2: Comparison with various RA element designs

Parameter design	Design 1 (Dreyer *et al*., 2014)	Design 2 (Chen *et al*., 2013)	Design 3 (Vosoogh *et al*., 2014)	Proposed design
Element design	Ring patch with variable size	Circular with ring I-shaped	Multi variable square ring	Triangular loop
Phase range	<326°	More than 360°	More than 360°	360°
Bandwidth	-	15.2%	17%	17.5%
Frequency band	X-band	X-band	K_u-band	K_u-band

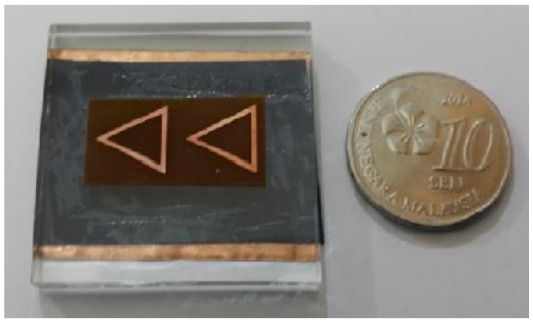

Fig. 7: Prototype of the element

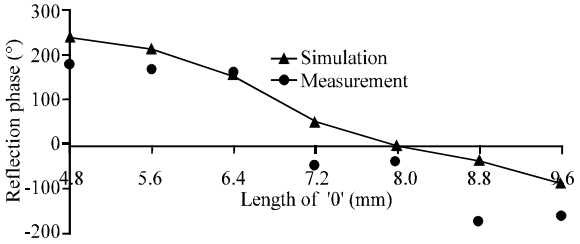

Fig. 8: Measured and simulated reflection phase at 13.7 GHz

RESULTS AND DISCUSSION

Validation: An element of 2×1 arrays was designed, fabricated and tested to validate its performance. The element as depicted in Fig. 7 was measured using a standard waveguide operating at both X and K_u bands which was connected directly to a Performance Network Analyzer (PNA). The obtained scattering data was then analyzed and compared with the simulated result. Figure 8 shows a comparison of linear phase range between simulation and measurement results. It is found that the linear phase range for both simulation and measurement methods exhibits more than 300° which is better compared to the research reported in Dreyer *et al*. (2014). More comparison on different parameter of each design can be seen in Table 2. These results also, indicate that the optimization process towards the triangular loop element has improved the bandwidth of 3% to be 17.5%. In addition, it is noted that the phase range from measurement results are in line with the simulation results. Graph as depicted in Fig. 9 showed the measured data comes with relatively enormous loss. The average loss is approximately 3.4 dB. These losses are sourced from the poor manufacturing and measurement processes where

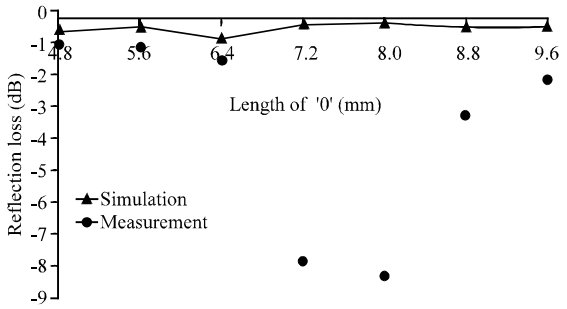

Fig. 9: Measured and simulated losses at 13.7 GHz

there are many weaknesses that cannot be avoided (Nguyen *et al*., 2015). Defects during etching process, improper system connection (limited number of connectors and devices) inexperience operator, etc. are among the weaknesses that contributed to this problem.

CONCLUSION

Simple triangular loop elements have been designed as a radiating element on a monocrystalline silicon cell. It has been demonstrated that the modification to the triangular loop element has increased the bandwidth over 17%. It is also, demonstrated from the measurement result that the employed element design can achieved wide phase range of about 326° for solar RA antenna. Moreover, the design can operate at dual frequencies within K_u-band.

ACKNOWLEDGMENT

This research was funded by Universiti Kebangsaan Malaysia under grant no. DIP-2015-014.

REFERENCES

Carrasco, E., M. Barba and J.A. Encinar, 2006. Aperture-coupled reflectarray element with wide range of phase delay. Electron. Lett., 42: 667-668.

Chen, Q.Y., S.W. Qu, J.F. Li, Q. Chen and M.Y. Xia, 2013. An X-band reflectarray with novel elements and enhanced bandwidth. IEEE. Antennas Wirel. Propag. Lett., 12: 317-320.

Dreyer, P., M. Morales-Masis, S. Nicolay, C. Ballif and J. Perruisseau-Carrier, 2014. Copper and transparent-conduc tor reflectarray elements on thin-film solar cell panels. IEEE. Trans. Antennas Propag., 62: 3813-3818.

Encinar, J.A. and J.A. Zornoza, 2003. Broadband design of three-layer printed reflectarrays. IEEE. Trans. Antennas Propag., 51: 1662-1664.

Li, J.F., Q. Chen, Q.W. Yuan and K. Sawaya, 2011. Reflectarray element using interdigital gap loading structure. Electron. Lett., 47: 83-85.

Li, L., Q. Chen, Q. Yuan, K. Sawaya and T. Maruyama *et al*., 2009. Novel broadband planar reflectarray with parasitic dipoles for wireless communication applications. IEEE. Antennas Wirel. Propag. Lett., 8: 881-885.

Misran, N., R. Cahill and V.F. Fusco, 2003.. Concentric split ring element for dual frequency reflectarray antennas. Electron. Lett., 39: 1-2.

Nguyen, B.D., K.T. Pham, V.S. Tran, L. Mai and N. Yonemoto, 2015. Reflectarray element using cut-ring patch coupled to delay line. IEEE. Antennas Wirel. Propag. Lett., 14: 571-574.

Oh, S.W., C.H. Ahn and K. Chang, 2009. Reflectarray element using variable ring with slot on ground plane. Electron. Lett., 45: 1206-1207.

Ramli, M., A. Selamat, N. Misran, M.F. Mansor and M.T. Islam, 2014. Dual configurations reflectarray element in improving dynamic phase range and loss. Intl. J. Appl. Eng. Res., 9: 23707-23716.

Vosoogh, A., K. Keyghobad, A. Khaleghi and S. Mansouri, 2014. A high-efficiency K_u-band reflectarray antenna using single-layer multiresonance elements. IEEE. Antennas Wirel. Propag. Lett., 13: 891-894.

Zawadzki, M. and J. Huang, 2000. Integrated RF antenna and solar array for spacecraft application. Proceedings of the 2000 IEEE International Conference on Phased Array Systems and Technology, May 21-25, 2000, IEEE, Dana Point, California, pp: 239-242.